ELSEVIER

Coordination Chemistry Reviews
159 (1997) 9–40

COORDINATION CHEMISTRY REVIEWS

Developments in laser selective spectroscopy and photophysics of d^6 metal–(di-imine) complexes

Elmars Krausz *, Hans Riesen

Research School of Chemistry, The Australian National University, Canberra, ACT 0200, Australia

Received 22 December 1995

Contents

Abstract

A brief introduction to laser selective spectroscopy is presented. The power of these techniques in being able to clearly elucidate the nature of electronic excitations and photophysical processes in the title complexes is provided by a number of examples. Included in the discussion are the determination of $g=2$, $S=1$ nature and zero field splittings of $^3\pi$–π^* luminescent states, direct measurements of excitation localisation and intramolecular excita-

* Corresponding author. Fax: 61-6-249-0750. E-mail: krausz@rsc.anu.edu.au

PII S0010-8545(96)01304-5

tion transfer in ^{3}MLCT states of ruthenium complexes and mini-exciton behaviour in osmium complexes. An important conclusion is that the intensities of sharp vibrational sideline patterns are variable and cannot be easily used to argue for or against excitation localisation. Far better is the study of electronic origins. The phenomenon termed nanoheterogeneity, where in addition to each chromophore having a distinct environment, each ligand or metal–ligand subunit experiences an independently distinct environment, has important consequences in amorphous environments. © 1997 Elsevier Science S.A.

Keywords: Laser selective spectroscopy; Nanoheterogeneity; d^6 metal–diimine complexes

1. Introduction

The photophysics, photochemistry and spectroscopy of metal-tris(di-imine) complexes, where $[Ru(bpy)_3]^{2+}$ (bpy = 2,2'-bipyridine) is undoubtedly the archetypal example, have been the subject of a great number of studies. There remains an ongoing conjunction of a chemical tunability and variability, as exampled by recent supramolecular syntheses [1] with spectroscopic applications, as exampled by laser selective spectroscopic measurements [2], for this very important class of complexes.

Laser selective spectroscopy in particular has been able to address directly, not only questions regarding the nature of the excited electronic states, their intensity mechanisms and intramolecular photophysical processes, but also the critical influence of what we term nanoheterogeneity on measurements made in amorphous environments. Energies of distinct ligand sections of a multi-ligand chromophore are not correlated; their energies vary independently in an inhomogeneous environment. The recognition of this effect allows a qualitative analysis of systems that appear to be dual emitters, without recourse to non-thermalisation of excited states.

The chemistry, photochemistry and spectroscopy of the title systems have been the subject of a number of reviews [3–10]. The purpose of this article is to provide an overview of some key developments in the spectroscopy and photophysics of these systems over the last five years, concentrating in the main on our own contributions.

2. Introduction to laser selective spectroscopy

Visible spectroscopy provides direct access to the range of electronically excited states in molecules and ions. In excited states, chemical and/or physical transformations and processes occur on a wide range of timescales. Laser-based techniques allow the measurement of electronic spectra with remarkable resolution and sensitivity, approaching the most fundamental limitations. These enhanced techniques can provide valuable and unique information regarding chromophoric species.

2.1. Homogeneous and inhomogeneous broadening

By comparison to NMR spectra, optical spectra taken in solution rarely show much detail and commonly appear as broad and featureless. In the solid phase,

optical spectra may sharpen, whereas NMR spectra (although intrinsically sharper) become broader relatively.

Electronic transitions involve a rearrangement of the electronic charge. The low mass of electrons means this occurs very rapidly. An electron in a molecule can be thought of as travelling an atomic radius distance in less than 10^{-15} s. The absorption of light provides "snapshots" of a molecule. As each individual molecule interacts with its environment, its precise electronic excitation energy is varied. An overall spectrum, corresponding to many absorption events, becomes smeared. NMR is, by comparison, far slower and the analogous fluctuations of the magnetic field at a nucleus during molecular motions are effectively averaged to a single, very well-defined value. Spectra then become well resolved.

This motional averaging in NMR is not active in rigid phases and the situation becomes similar to that which is always apparent in optical spectroscopy. Each species is in a unique and slightly different microenvironment. There is a corresponding spread of excitation energies giving rise to inhomogeneous broadening. Inhomogeneously broadened spectra commonly (but not always) have a Gaussian line shape (see Fig. 1).

Excited states decay by radiative and non-radiative processes. The radiative lifetime (τ) is inversely proportional to the absorption strength as measured by the integrated molar extinction. Radiative lifetimes have a value around 1 ns for strongly allowed (π–π^*) electronic transitions. Weakly allowed transitions, such as spin-forbidden d–d transitions in metal systems, have radiative lifetimes 10^6 times longer (ms).

The lifetime of any excited state gives rise to a homogeneous lineshape. The homogeneous lineshape is Lorentzian (the Fourier transform of the lifetime) with a linewidth given by $\Gamma_h = 1/2\pi\tau$ at $T=0$. An important consideration is that even for the most intense, fully allowed transitions, the homogeneous linewidth is less than 1 GHz but for weaker transitions Γ_h may be less than 1 kHz! The conversion factor

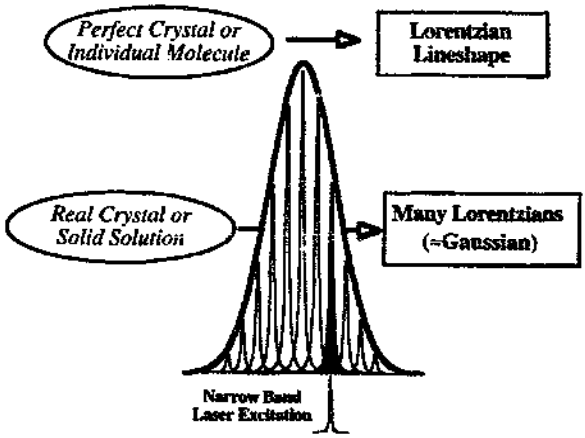

Fig. 1. Schematic representing the principle of laser selective spectroscopies.

is 30 GHz↔1 cm^{-1}. The inhomogeneous component ($\approx$1–1000 cm^{-1}) dominates linewidths seen in real systems in general by many orders of magnitude.

2.2. *Fluorescence line narrowing and hole burning*

It is possible to overcome some of the limitations of inhomogeneously broadened spectra in the solid state by using narrow band laser excitation. Single-frequency ring lasers or even inexpensive, semiconductor diode lasers are tunable over a significant wavelength range and can have linewidths less than 1 MHz. This corresponds to a resolving power of more than 1 in 10^8.

If one excites an inhomogeneously broadened ensemble of chromophores with a narrow band laser, only those species that are resonant (to within the homogeneous linewidth) with the laser frequency are excited. If the chromophore fluoresces, the fluorescence will narrow via this selectivity. This phenomenon is called fluorescence line narrowing (FLN) and is illustrated in Fig. 2.

A complementary method of overcoming inhomogeneous broadening is via spectral hole-burning. A narrow band laser is tuned to be within the inhomogeneously broadened absorption profile of a chromophore. With only modest laser power, one can significantly deplete the number of molecules absorbing at the laser frequency, thereby creating a spectral hole in the absorption spectrum at the laser wavelength. The depletion can come about in three main ways.

(1) Transient holes are created when an excited state of the molecule with a long lifetime creates a bottleneck in the process of returning to the ground state. A depletion in the number of absorbing molecules occurs.

(2) Photochemical holes are formed when the excited state molecule forms a

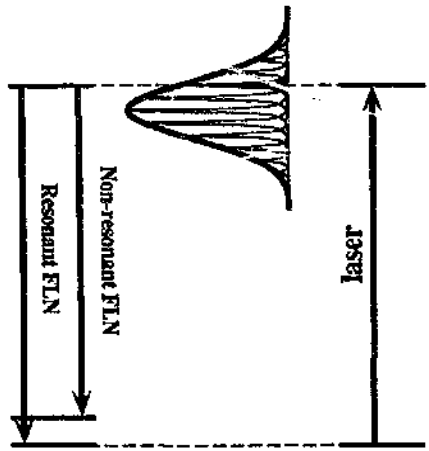

Fig. 2. Schematic of the fluorescence line narrowing (FLN) technique. This is usually given as a generic term to include phosphorescence and luminescence narrowing.

stable photoproduct. This new species absorbs at wavelengths different from the starting molecule.

(3) Photophysical hole burning involves a subtle rearrangement of host–guest interactions (Fig. 3). Spontaneous hole filling in the ground state can be much slower and a depletion of the number of molecules absorbing at the laser frequency is created.

Photophysical holes can persist indefinitely at low temperatures. The two-level system (TLS) model (Fig. 3) is used to describe this fascinating process which is measurable for many chromophores at low temperatures.

The ability to observe extremely narrow spectral features from FLN or hole-burning experiments facilitates a great range of experiments on chemically interesting and important systems. A great deal of spectral and kinetic information can be gleaned. We have written an introduction [2] to these spectroscopies, specifically for chemists, using a wide range of examples from our own work.

3. Excitons and electronic structure; d–d, π–π^* and MLCT excited states

Metal di-imine complexes with π acceptor ligands such as bpy and 1,10-phenanthroline (phen) show characteristically ligand-centred π–π^* excitations in the near-UV which are analogous to excitations of the free ligand. Intense metal to ligand charge transfer (MLCT) absorption features appear in the visible spectrum, associated with an electron being transferred from an accessible metal d orbital into the (ligand) π^* system. The qualitative molecular orbital description for tris complexes shown in Fig. 4 is well known. Thicker arrows indicate orbital excitations that are expected to be strongly allowed and the MLCT absorption spectra are expected to show the consequences of the splitting in the ligand orbitals.

The electronic configuration of the series Fe^{2+}, Ru^{2+}, Os^{2+} has a d^6 configuration

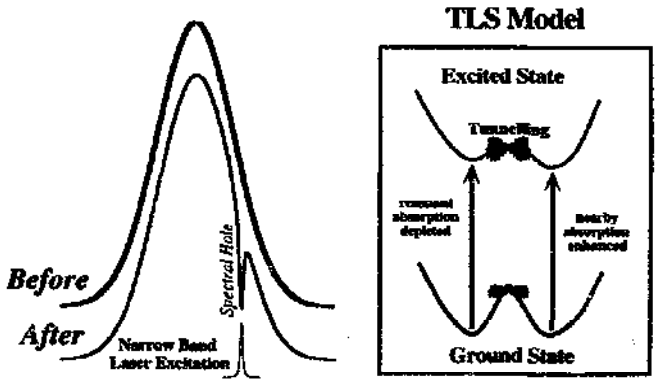

Fig. 3. Schematic of hole burning and the two-level system (TLS) model of photophysical hole burning.

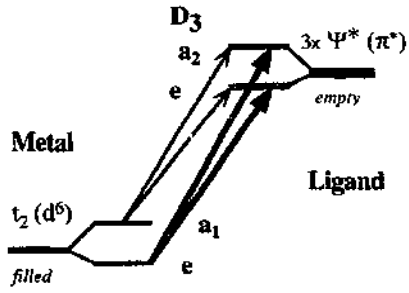

Fig. 4. Orbital scheme of tris di-imine complexes.

with the spin–orbit coupling parameter λ increasing significantly from about 400 to 1000 to 3000 cm^{-1}. The octahedral component of the crystal field energy (10 Dq) is about 20 000 cm^{-1} for the ruthenium complex. A strong crystal field gives rise to a filled t_2 subshell of the d electron manifold in the ground state on the metal centre of the chromophores. The t_2 (octahedral) orbital symmetry is further split at about 300–500 cm^{-1} by the trigonal component of the ligand field (Fig. 4). The lowest acceptor π^* orbital of bpy is calculated to be antisymmetric (with respect to the two aromatic rings) and labelled Ψ^*.

In the absence of interligand coupling, the acceptor orbitals on the three ligands have the same energy. The coupling, often termed exciton coupling, gives rise to a splitting with resultant orbitals of a_2 and e symmetry (Fig. 4). The π^* orbital splitting has been most recently calculated at about 1400 cm^{-1} from ab initio density functional calculations [11] on $[Ru(bpy)_3]^{2+}$. The magnitude of this splitting, which does not depend strongly on the metal centre, is in accord with many previously determined values made at a lower level of calculation. In the density functional-based calculation, the lowest energy ^{3}MLCT multiplet, which according to the calculation is of ^{3}A symmetry, is split by about 20 cm^{-1}.

It was suggested some time ago [12,13] that the circular dichroism (CD) observed in the π–π^* region in the title systems could be accounted for by an exciton coupling mechanism, specifically involving dipole–dipole coupling of ligand excitations. To account for the CD, an exciton coupling parameter of $\beta \approx 900$ cm^{-1} was required which is in reasonable agreement with a value calculated from dipole–dipole coupling. Related processes have been suggested to be responsible for CD in the ^{1}MLCT region. Fig. 5 illustrates the ligand-centred and MLCT exciton basis states.

An experimental investigation [14] of the interligand interactions in the π–π^* states indicates $|\beta|$ to be less than 100 cm^{-1} This was made from a comparison of heteroleptic complexes (typically complexes with both bpy and phen ligands). Not only is this coupling far less than predicted by the exciton dipole–dipole coupling model but it is of opposite sign to that needed to account for the CD. Circular dichroism in the π–π^* state was then attributed to a vibronic coupling process. The CD of ^{1}MLCT states has, again from an experimental study of families of complexes, been determined [4] as arising from a metal-centred magnetic dipole process. The

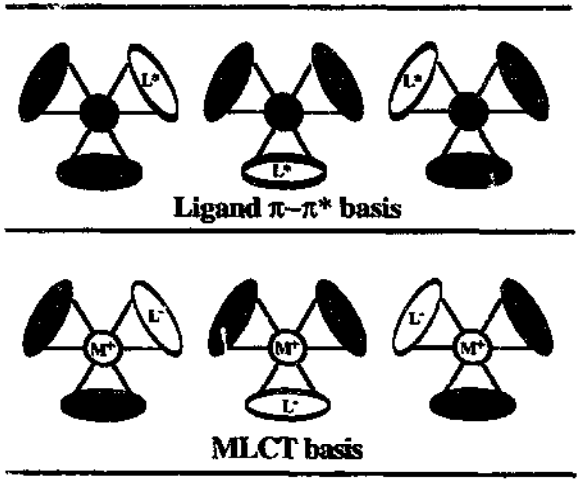

Fig. 5. Schematic of exciton basis states for tris di-imine complexes.

exciton coupling process was again excluded as a source of the CD activity in the MLCT case.

There are unresolved difficulties [15] in reconciling the CD, MCD and polarised absorption spectra in the ^{1}MLCT region with a theoretical model of the chromophores. The overall assignments and associated intensity processes are not yet understood. However, there is evidence [16] that excitation interaction in the spin-allowed ^{1}MLCT region is not much greater than about 200 cm^{-1}. Coupling in the spin-forbidden ^{3}MLCT and $^3\pi$–π^* states is naturally expected to be considerably less. As an initial measure, one could expect the interaction to scale roughly with the dipole strength. In the analysis of MLCT absorption spectra developed by Ferguson and Herren [17] it was indeed necessary to set the effective interaction parameter between the ligands in the triplet states to zero in order to account for spectral properties.

An incisive probe of interactions in the ^{3}MLCT state was made by Riesen et al. [18]. They were the first to prepare complexes in which one or more of the bpy ligands were perdeuterated (bpy-d_8), thus subtly breaking the trigonal symmetry of the complex. Deuteration of all three ligands blue shifted the origins of ^{3}MLCT excitations by about 40 cm^{-1}. Notably, complexes with one or two deuterated ligands showed two sets of origin features, corresponding to excitations of deuterated and non-deuterated metal–ligand subunits. These and analogous experiments with mixed ligand complexes have since established (see following sections) that the intramolecular excitation coupling in Ru(II) complexes is less than 0.1 cm^{-1}. The coupling remains, however, sufficient to allow thermal equilibrium between excitations on adjacent metal–ligand units. In analogous osmium complexes, the ^{3}MLCT origins are considerably more intense, and coupling between metal–ligand subunits becomes significant and measurable.

4. $^3\pi$–π^* Luminescent states

An attractive feature of the title class of complex is that, by varying the ligand or replacing the metal, etc., it is possible to prepare systems in which the relative energies of the MLCT, d–d and π–π^* excitations can be tuned at will. Families of complexes can be found in which either a ^{3}MLCT, $^3\pi$–π^* or a d–d state is lowest and thus responsible for the luminescence, photophysics or photochemistry.

4.1. Direct observation of g = 2, S = 1 *behaviour*

There have been difficulties in discriminating between ^{3}MLCT (metal–ligand) and $^3\pi$–π^* (ligand-centred) assignments of luminescent states in a number of examples. Indirect evidence such as lifetime data, Stokes shifts, luminescence bandshapes or chemical systematics is often used but can be misleading. Section 5.1 provides what we feel is a remarkable example of such a situation. The most characteristic property of an MLCT state is, quite naturally, its excited state electric dipole moment and a definitive assignment of such states has come only recently for ^{3}MLCT states from single crystal high-resolution Stark measurements (see Section 5.3). Charge transfer assignments for ^{1}MLCT transitions have been vindicated by electrochromism [19,20] measurements.

The corresponding, most characteristic property of a $^3\pi$–π^* excited state is its (spin-only) magnetic moment. Resonant FLN experiments performed in the presence of an applied magnetic field have been able to definitively and unambiguously assign [21–25] luminescence arising from a $^3\pi$–π^* excited state. The five-line pattern shown for the example of $[Ir(phen)_3]^{3+}$ in an ethanol/methanol glass in Fig. 6 has the signature spacing corresponding to a $g=2$, $S=1$ spin triplet state and leaves no doubt regarding an assignment. Five lines are seen from the triplet in the narrowing experiment as the laser can excite the $M_S=-1$, 0, or 1 sublevels. Relaxation processes within the lifetime of the excited states lead to each giving rise to two sidelines for each set. The overlapping of three sets of three lines gives rise to five equally spaced lines (for a simple triplet with negligible splittings at zero field) whose relative intensities vary with temperature.

4.2. Optical resolution of zero field splittings

Since the first observation of resonant Zeeman FLN [22] on the $^3\pi$–π^* luminescent state of $[Ru(i\text{-}biq)_3]^{2+}$ (i-biq = 3,3′-biisoquinoline) in amorphous environments, where the homogeneous linewidth was determined to be 260 MHz, it was clear that it should be possible to observe zero field splittings (ZFSs) in $^3\pi$–π^* states. ZFSs for free ligands are of the order of 1–5 GHz. The ZFS spacings, which are in the microwave frequency region, are usually probed by the optically deleted magnetic resonance (ODMR) technique. The emitting state of $[Rh(bpy)_3]^{3+}$ was assigned [26] as a $^3\pi$–π^* state using this method and ZFSs were shown to be comparable to those found in the free bpy.

We were able to observe [23,27] sidelines in the hole-burning spectrum of a rigid aromatic molecule (coronene) in an amorphous environment. ZFSs could then be

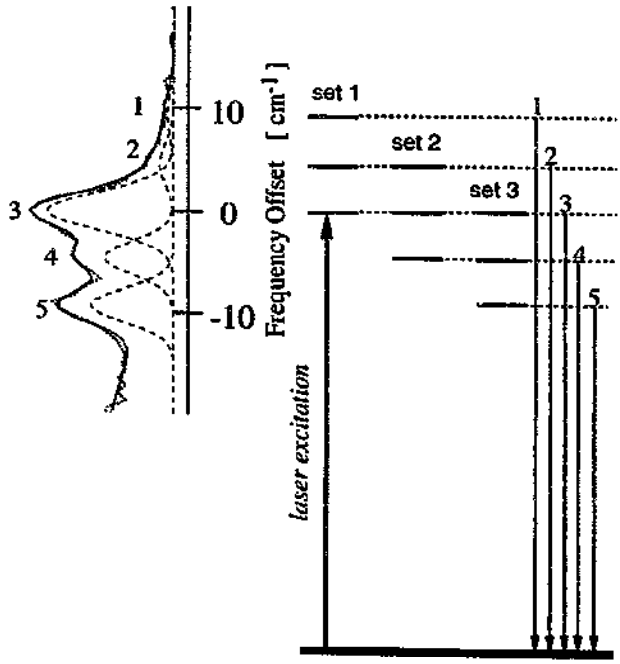

Fig. 6. The five-line pattern arising from the resonant FLN excited at 448 nm of $[Ir(phen)_3]^{3+}$ in 4:1 ethanol:methanol at 4.2 K and 5 T applied field. Adapted from [21].

directly determined for this case, but a range of other aromatic molecules and coordination complexes, although having very sharp central features in hole burning or FLN, had weak, broad, side features [21–25]. An analysis of these patterns established that the ZFSs are not well defined in amorphous environments for many systems. Laser selection excites the full range of complexes that absorb at the excitation wavelength. These have a large spread of ZFSs which gives rise to broad and correspondingly weak side structure as correlation between excitation energy and ZFS is characteristically poor.

The ODMR technique preferentially detects those particular complexes that have sublevels with widely differing luminescence lifetimes. If two triplet sublevels have similar lifetimes then no change in luminescence will be seen upon microwave pumping between sublevels and no ODMR signal is seen. ODMR is blind to such species but direct optical measurements such as FLN will see the two levels with equal intensity. Furthermore, in ODMR it is difficult to scan over a large frequency range with a constant sensitivity and thus the technique can easily provide misleading spectra when there is a quasi-continuum of ZFSs. Optical methods are characteristically very uniform in sensitivity and can also scan over far larger energy differences.

$[IrCl_2(5,6\text{-}Me_2phen)_2]^+$ provides an interesting example [25] of a system in which ^{3}MLCT and $^3\pi$–π^* lowest excited states are close to resonance. We were able to

confirm, through the observation of the distinctive five-line $g=2$, $S=1$ pattern, the ligand-centred nature of the luminescence. The ZFSs, though not well defined, were shown to be an order of magnitude larger (30 GHz) than the values obtained for free ligands. This was taken to reflect relatively strong interaction with nearby MLCT states. In the $[Rh(phpy)_2(bpy)]^+$ (phpy = phenyl pyridine) system [24], where there had been some speculation that interactions with MLCT states may have been significant, the ZFS was again uncorrelated and in the range of 9 GHz.

4.3. Dual emission and nanoheterogeneity

Luminescence usually arises from the lowest excited states in transition metal complexes unless the gaps between excited states are unusually large (>6000 cm^{-1}) or very small (< 1 cm^{-1}). In the normal course of events, fast radiationless and intersystem crossing processes ensure an effective thermal equilibrium amongst excited states. Thermal equilibrium in turn constrains luminescence intensities to have a simple first-order kinetic behaviour, that is they are "single" exponential.

There have been a number of reports of inorganic complexes whose properties have been interpreted as due to electronic excited states of different character [28–49] separated by energies well within the range of vibrational or lattice phonon energies (≈10–3000 cm^{-1}), but not in thermal equilibrium. These systems are characterised by the appearance of two distinct emissions, non-exponential decay kinetics and other anomalous spectroscopic features. The dual emitter concept has a rather wide acceptance in the inorganic chemistry community.

A common source of non-exponential kinetics in the luminescence of a dilute sample is impurities. Impurities may contribute to the overall luminescence without being easily detectable analytically. A fundamental difficulty arises from the fact that it is not possible to distinguish between a dual emitter and the presence of more than one emitting species in the sample, by most experimental procedures.

The $[Rh(bpy)_x(phen)_{3-x}]^{3+}$ series [41] in which the luminescence is of $^3\pi$–π^* character provides, for the mixed ligand complexes $x=1$ and 2, a classic example of dual emitter behaviour. Very strongly non-exponential decay kinetics are seen for the mixed ligand complexes, consistent with bpy and phen $^3\pi$–π^* emissions being independent. The fraction of each component of the luminescence follows the stoichiometry of the complex.

The $[Ir(bpy)_x(phen)_{3-x}]^{3+}$ series behaves entirely analogously (Fig. 7), but the lifetimes of the bpy and phen $^3\pi$–π^* luminescences are shortened with the spin–orbit coupling on third-row iridium(III). Consequently, it becomes feasible to resonantly excite into the $^3\pi$–π^* origin region of these complexes with a laser. In this spectral region the bpy ligand absorbs an order of magnitude more strongly than phen. An absence of characteristic phen luminescence at short times following short-pulse laser excitation in the origin regions of the mixed ligand complexes would provide indisputable evidence for the dual emission hypothesis. Any subsequent rise of phen luminescence would further quantify the kinetics of excitation transfer between the ligands. Luminescence with resonant excitation is, however, found to be not significantly different to that obtained with UV excitation into the π–π^* region, i.e. the

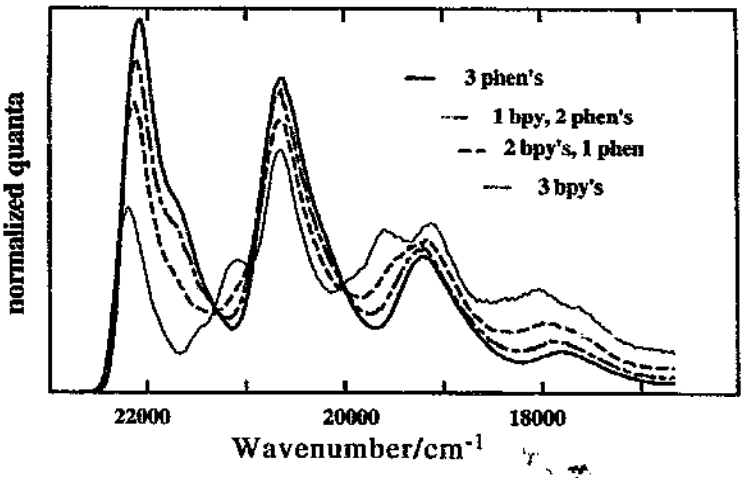

Fig. 7. Normalised luminescence spectra of the $[Ir(bpy)_x(phen)_{3-x}]^{3+}$ series in 4:1 ethanol:methanol at 4.2 K excited at 350 nm. Adapted from [50].

normal situation in spectroscopy. Dual emission does not occur [50] for the $[Ir(bpy)_x(phen)_{3-x}]^{3+}$ series.

One can quantitatively account for the data in Fig. 7 and lifetime data using a model in which the $^3\pi$–π^* excitations of the phen and bpy ligands have an inhomogeneous spread of 220 cm^{-1}, which is large compared to the average energy difference between bpy and phen excitations of 70 cm^{-1}. The key concept is that the excited state energies of the bpy and phen ligands are not correlated and vary independently (Fig. 8). In a significant proportion of the species in frozen solution, the bpys, which are on average at higher energy, are at lower energy. Poor correlations of electronic energy levels in coordination compounds in amorphous environments [51] was

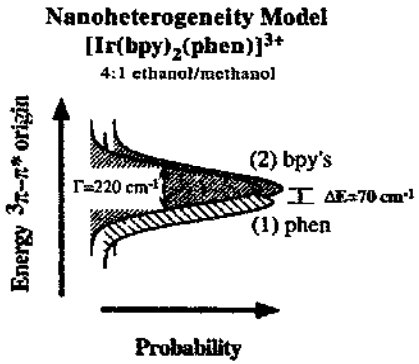

Fig. 8. Schematic of model used to qualitatively account for data in Fig. 7 and lifetime data. Adapted from [50].

suggested by measurements using laser selective spectroscopy (e.g. ZFSs in Section 4.2).

Phonon-assisted energy back transfer from the lowest energy ligand to a higher energy ligand may occur at a rate fast compared to the excited state lifetime at elevated temperatures. It may indeed be possible to observe this rate directly by the Lorentzian broadening of resonantly narrowed luminescence.

We re-examined [52] the luminescence characteristics of *cis*-$[Ir(bpy)_2Cl_2]^+$. The luminescence behaviour of this system in a range of frozen glasses is unusual and it was given to be a clear example of a dual emitter. By using variable wavelength excitation techniques at low temperatures, we discovered that this system is not a dual emitter with d–d and ^{3}MLCT states of the complex separated by about 400 cm^{-1} as reported, but that a much larger energy gap was probably operative.

Although dual emission is in principle possible in transition metal complexes, its likelihood is not great, as a vanishingly weak interaction between two excitation subunits can lead to a fast excitation transfer rate. A simple approach calculates that an interaction of 0.1 cm^{-1} gives rise to a transfer rate of about 10^9 s^{-1}. We know of no example of dual emission in transition metal complexes that has withstood close scrutiny. Recent work on dual emission of Re(I) complexes [49] is probably explicable in terms of nanoheterogeneity.

5. ^{3}MLCT luminescent states

The dramatic temperature dependence of the luminescence characteristics of ^{3}MLCT states is due to the presence of closely spaced emitting levels (noted generically as I, II and III for ruthenium complexes) that have transition dipole strengths differing by two orders of magnitude. Levels I, II and III are in thermal equilibrium and give rise to a single exponential decay at each temperature.

In the absorption and luminescence spectra of $[Ru(bpy)_3](PF_6)_2$ and, particularly, doped $[Zn(bpy)_3](ClO_4)_2$:Ru crystals, fine structure is observed in the spectra and it is possible to identify [53–59] purely electronic origins (see Fig. 9 [60]) associated with the lowest electronic levels I, II and III.

This fine structure is an order of magnitude stronger in the ClO_4 than in the PF_6 lattices. The energy level spacings are, however, similar. Independent values of the spacings obtained from the conventional analysis of the temperature dependence of the luminescence lifetimes agree well [61].

5.1. $[Ir(bpy)_2(acac)]^{2+}$ and $[Ir(bpy)_2(MeOH)]^{3+}$

These complexes (MeOH = methanol, acac = acetylacetonate) [61] have luminescence spectra in ethanol/methanol glasses almost indistinguishable from that of $[Ir(bpy)_3]^{3+}$ (Fig. 10). On this basis and from the knowledge that the ^{1}MLCT absorption features lie at high energy in these systems, a $^3\pi$–π^* assignment seems completely straightforward. They do, however, show exponential luminescence decays with short ($\approx$10 μs) lifetimes at 77 K, compared to the value of about 50 μs for $[Ir(bpy)_3]^{3+}$. The decay profile of $[Ir(bpy)_3]^{3+}$ becomes non-exponential at low

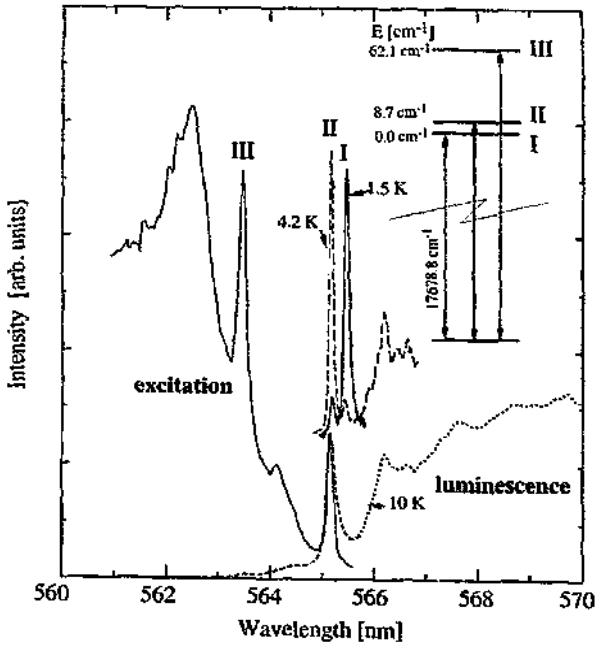

Fig. 9. Origins I, II and III of $[Zn(bpy)_3(ClO_4)_2]$:Ru in non-resonant luminescence and excitation spectra. Adapted from [60].

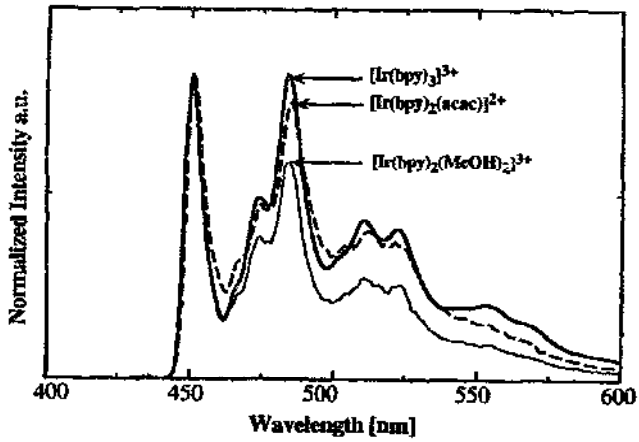

Fig. 10. Normalised luminescence spectra of the Ir(III) complexes indicated in 4:1 ethanol:methanol at 4.2 K, excited at 350 nm.

temperatures (a consequence of the ZFSs of about 0.1 cm^{-1} in $^3\pi$–π^* states). The luminescence decays of the $[Ir(bpy)_2(acac)]^{2+}$ and $[Ir(bpy)_2(MeOH)]^{2+}$ complexes remain single exponential and show the strong temperature dependence so characteristic of ^{3}MLCT emitters with a lifetime at the lowest temperatures approaching 200 μs.

Resonant FLN spectra as a function of temperature and magnetic field are definitive. In the absence of a magnetic field a single side feature was seen, displaced by 8 cm^{-1} for the MeOH complex and 15 cm^{-1} for the acac complex. In an applied magnetic field the spacings increased but the five-line pattern with separations of $2\beta B$ was *not* observed. The narrowed spectra in the title compounds are characteristic of a ^{3}MLCT luminescent state.

5.2. *High-symmetry host lattices*

Inhomogeneous broadening is, in general, less prominent in crystalline environments. The most spectroscopically useful lattices have a small number of appropriate sites of high symmetry into which a chromophore can be introduced and have minimum inhomogeneous broadening. Detailed studies of such systems have been critical in the promotion of our understanding of the spectroscopy of the title complexes. Concepts developed from detailed measurements in crystal lattices can be used to understand the obscured and variable spectroscopy of the same species in amorphous environments.

One difficulty is that high-symmetry lattices are prone to symmetry breaking and phase changes. This can lead to multiple sites or disorder and severe inhomogeneity. One very useful high-symmetry lattice is racemic $[Ru(bpy)_3](PF_6)_2$. This $P\bar{3}c1$ structure preserves the inherent D_3-32 symmetry of the cation [62]. At room temperature there is one site. A phase change occurs around 190 K and while the crystal symmetry remains trigonal, the unit cell triples to form the space group $P31c$, the old tertiary axes becoming the new secondary axes. The structural modulation consists of about 3° relative rotations of $[Ru(bpy)_3]^{2+}$ units about their threefold axes giving rise to three inequivalent sites [63] in the asymmetric unit, each of C_3-3 symmetry. A spectroscopic probe of the three sites was made [64] by doping the crystal with $[Os(bpy)_3]^{2+}$. Site-selective luminescence spectra identified three sites spaced by about 40 cm^{-1}. Microcrystal absorption spectra [16] of the undoped material have been used to identify ^{3}MLCT origins II and III of the three $[Ru(bpy)_3]^{2+}$ sites which are spaced by about 40 cm^{-1}.

It is of great practical advantage in spectroscopic studies to have a transparent isomorphous crystal host in which one can dope a chromophore. Problems associated with intermolecular energy transfer and interaction, as well as high optical density samples, can be circumvented. We have tried to identify a transparent lattice that preserves the full symmetry of tris(bpy) complexes without success.

By far the most useful lattices have been racemic $[M(bpy)_3](ClO_4)_2$ (M=Zn and Ru). Both crystallise [16,65–67] in the monoclinic space group $C2/c$ with four formula units per unit cell. The structure can be described as a commensurate modulation of an idealised structure of $P\bar{3}c1$. Cations are equivalent and their symmetry is C_2-2. No phase change occurs upon cooling as these salts are locked

into a tight, modulated structure at room temperature. Inhomogeneous broadening in these lattices is small but somewhat dependent upon growth conditions.

Within a single cation, one bpy lies on the symmetry axis (*b* axis, Fig. 11) while the other two bpys are equivalent. Bite angles and bond lengths are very similar for all three bpys but the distinct ligand has a different ClO_4 environment. As a consequence, MLCT transitions to the distinct ligand L_a lie 300–700 cm^{-1} higher in energy than corresponding transitions involving the crystallographically equivalent ligands $L_{b,\,b'}$. An energy difference of about 2000 cm^{-1} is calculated [68] by a point charge model. The inequivalence manifests itself in a strong dichroism [16] in the metal–ligand plane.

One very important consequence of the *C*2/2 symmetry of this lattice is that heteroleptic complexes of the type $[M(bpy)_{3-x}(L)_x]^{2+}$ can enter the lattice in the two ways shown in Fig. 12. If one chooses a ligand L such as 3,3'-bipyridazine (bprid) or 2,2'-bipyrazine (bpz) to which MLCT is far (about 3000 cm^{-1}) less energetic than bpy, the $x=1$ material shows [69–71] two overlapping luminescence spectra. These arise from the L ligand in the one distinct and two equivalent positions provided by the host. For M=Ru and L=bprid, this energy difference is 360 cm^{-1} and the intensity ratio of the two emissions at high temperatures simply reflect the statistics of one distinct and two equivalent positions.

5.3. Stark splittings, high resolution and transient hole burning

The enhanced intensity in the electronic origins, low inhomogeneous broadening and other helpful properties of the ClO_4 lattices have allowed a number of incisive experiments to be performed on ^{3}MLCT states. These include Stark, Zeeman and truly high-resolution experiments [60,65,72,73] on $[Ru(bpy)_3]^{2+}$.

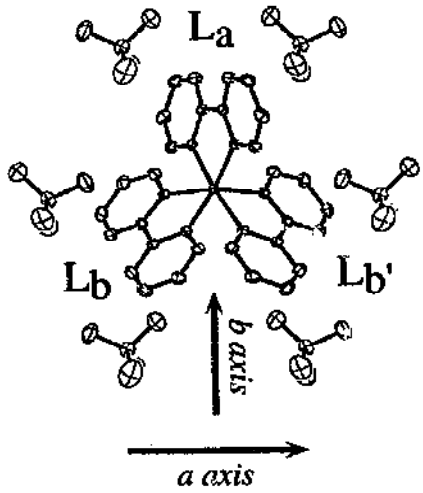

Fig. 11. Crystal structure with anion environment for racemic $[Ru(bpy)_3(ClO_4)_2]$. Adapted from [16].

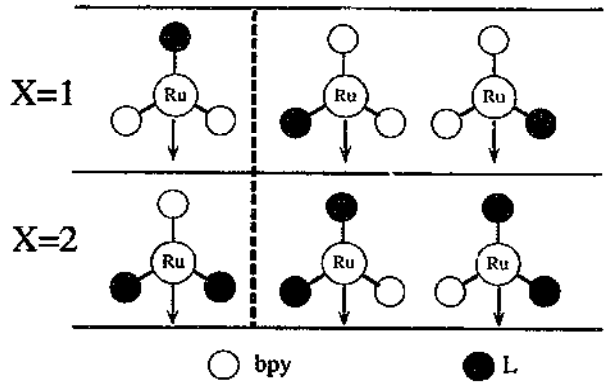

Fig. 12. Schematic of how the heteroleptic complexes $[Ru(bpy)_{3-x}(L)_x]^{2+}$ may substitute in the $C2/c$ $[Zn(bpy)_3(ClO_4)_2]$ lattice.

FLN and the important complementary excitation line narrowing experiments establish that MLCT excitations are very strongly localised on a single metal–ligand subunit. Stark experiments quantify that levels I, II and III are indeed charge transfer in character and have a dipole moment of 5.5 D. The application of an electric field perpendicular to the crystal b and c axes (Fig. 13) shifts MLCT excitations of $Ru–L_b$ and $Ru–L_{b'}$ subunits to different energies. A doubling of origin features ensues (Fig. 14) from which the dipole moment can be calculated. The doubling of

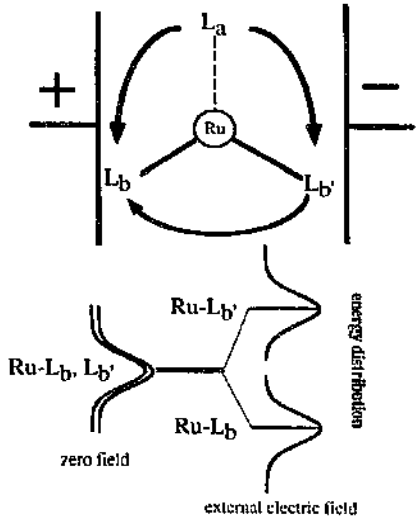

Fig. 13. Schematic of a Stark experiment in $[Zn(bpy)_3(ClO_4)_2]$:Ru. Arrows indicate fast excitation transfer from the higher energy $Ru–L_a$ subunit and between the $Ru–L_b$ and $Ru–L_{b'}$ subunits. Excitation of the latter subunits becomes inequivalent in an applied electric field.

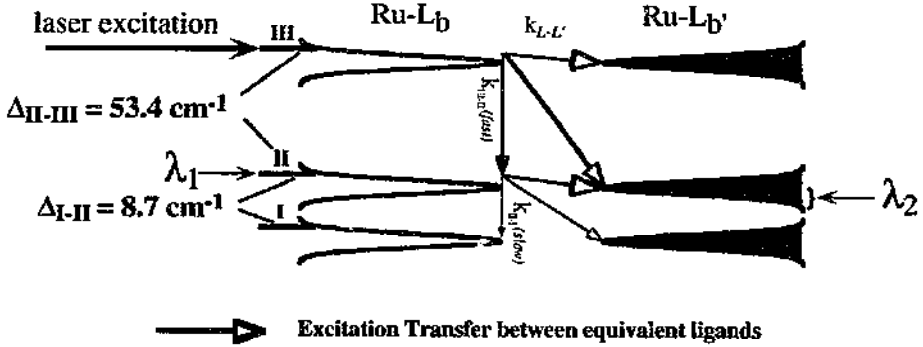

Fig. 15. Schematic of excitation transfer experiment in the lowest energy excitations in $[Zn(bpy)_3(ClO_4)_2]$:Ru. Laser excitation selects level III at a high energy within the inhomogeneously broadened distribution. This gives rise to well-defined energies of II and I on Ru–L_b. Subsequent excitation transfer to Ru–$L_{b'}$ leads to emission from a broader and slightly lower energy distribution of II and I levels (see text).

experiments also establish that there are no ZFSs in this system in the range 1–3 GHz as has been suggested [74–77] by ODMR experiments. Sublevels would have been readily detected as sidelines in our FLN experiments.

Stark-swept transient hole-burning experiments [60] on this system are made feasible by a conjunction of a number of the properties mentioned above. An upper limit for the homogeneous linewidth of about 15 MHz (=0.0005 cm^{-1}) was obtained by bringing transiently selected chromophores in and out of resonance with a narrow band laser via an applied electric field of just 10 V cm^{-1}. The lifetime of level I is about 200 μs and thus too long be responsible for the observed width. The 15 MHz linewidth observed limits intramolecular excitation energy transfer (between Ru–L_b and Ru–$L_{b'}$) to be slower than about 10 ns, suggesting the experiment described in Section 5.7.

5.4. Selective deuteration

For π–π^* excitations of aromatic molecules, a gradual energy shift of origin features as a function of the degree of deuteration of the molecule is routinely observed. This type of electronic excitation is delocalised over the entire chromophore. Naphthalene, for example, has a linear shift of about 15 cm^{-1} per deuteron. A corresponding gradual shift of origin features to higher energy upon progressive deuteration of the ligands would be expected if ^{3}MLCT were delocalised over three ligands.

Fig. 16 shows the excitation and luminescence spectra in the region of the lowest-energy electronic origins for the $[Ru(bpy)_{3-x}(bpy\text{-}d_8)_x]^{2+}$ (x=0 to 3) series in the favourite $[Zn(bpy)_3](ClO_4)_2$ lattice [78]. A comparison of the spectra of the perprotonated (x=0) and perdeuterated (x=3) complexes show that origins I, II and III undergo a 40 cm^{-1} blue shift upon perdeuteration. Two sets of electronic origins I,

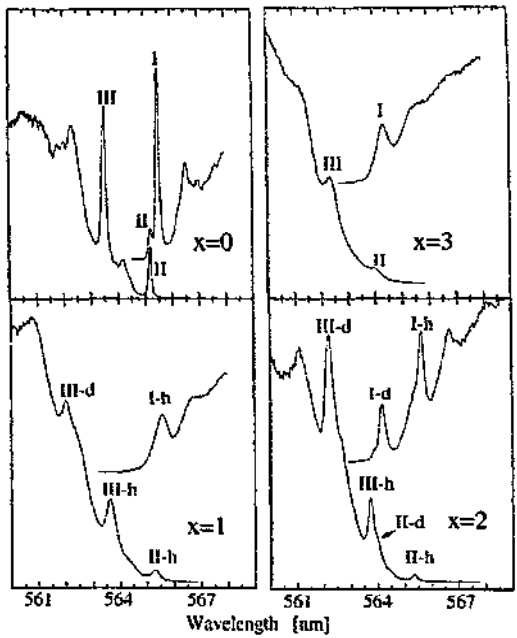

Fig. 16. Non-resonantly excited excitation and luminescence spectra of the series $[Ru(bpy)_{3-x}(bpy\text{-}d_8)_x]^{2+}$ in $[Zn(bpy)_3(ClO_4)_2]$. Adapted from [78].

II and III are observed in excitation for the $x=1$ and $x=2$ systems. These are clearly associated with localised excitations involving the Ru–bpy and Ru–bpy-d_8 subunits as they occur at the positions of the origins in the $x=0$ and $x=3$ materials respectively. It follows that excitation exchange interaction between Ru–bpy subunits must be far smaller than the deuteration energy shift of the origins (40 cm^{-1}).

In the $x=2$ system, luminescence associated with the Ru–bpy-d_8 subunit, identified by origins I-d and II-d, occurs for 1/3 of substitutions (both crystallographically equivalent bpys are substituted by bpy-d_8 see Fig. 12). When this occurs, excitations of the remaining (Ru–bpy) subunit will involve the distinct bpy position lying at higher energy which cannot trap the luminescence via intramolecular excitation transfer. In the $x=1$ system, excitation transfer ensures that luminescence will invariably involve an Ru–bpy subunit as each Ru–bpy-d_8 subunit which has a ligand in the equivalent position must have a (lower energy) Ru–bpy partner.

Distinctly different behaviour is provided [3,79,80] by the series $[Ru(bpy\text{-}d_x)_3]^{2+}$ ($x=0$, 2, 6, 8). Here a simple linear shift is observed with no doubling of origins. Clear confirmation for our assignments [80] is found in the $[Ru(bpy)(bpy\text{-}d_6)_2]^{2+}$ and $[Ru(bpy\text{-}d_2)(bpy\text{-}d_8)_2]^{2+}$ systems. The origins of the *Ru–bpy-d_6* and Ru–bpy-d_2 subunits shift to lower and higher energy, respectively, in comparison with the transitions involving the Ru–bpy-d_8 and Ru–bpy subunits in $[Ru(bpy)(bpy\text{-}d_8)_2]^{2+}$. They align well with origins of $[Ru(bpy\text{-}d_6)_3]^{2+}$ and

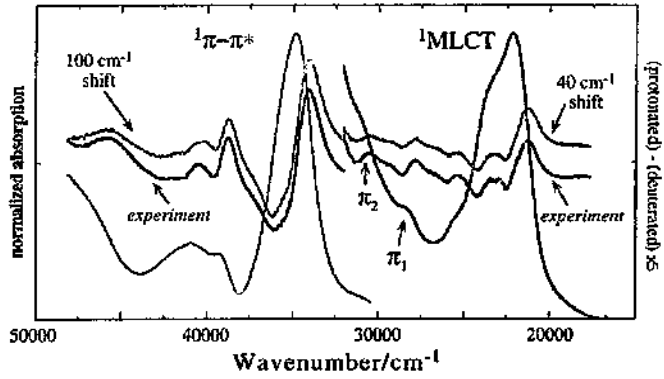

Fig. 17. Normalised room temperature solution spectra of $[Ru(bpy)_3]^{2+}$ in ligand-centred (UV) and MLCT (visible) regions. Differential curves show the experimental shift of the spectra upon deuteration of the complex along with (offset) curves derived from simple 40 and 100 cm^{-1} blue shifts of the absorption spectrum. Weak features marked π_1 and π_2 have the shift of π–π^* rather than MLCT excitations.

$[Ru(bpy\text{-}d_2)_3]^{2+}$. Origins of the Ru–bpy and Ru–bpy-d_8 subunits in $[Ru(bpy)(bpy\text{-}d_6)_2]^{2+}$ and $[Ru(bpy\text{-}d_2)(bpy\text{-}d_8)_2]^{2+}$ align with the origins in $[Ru(bpy)(bpy\text{-}d_8)_2]^{2+}$. An additivity of origin features is maintained.

FLN and excitation line narrowing experiments of the series $[Ru(bpy)_{3-x}(bpy\text{-}d_8)_x]^{2+}$ ($x=0$ to 3) demonstrate, in a compelling way, the independence of the ^{3}MLCT transitions of the two crystallographically equivalent ligands. When both crystallographically equivalent ligand positions are occupied by identical ligands (i.e. both deuterated or both protonated but not one of each) the intensity ratio between the narrowed and broad feature (see previous section) is simply 1:1. Most importantly, the broad feature is entirely absent when the equivalent ligand position is occupied by a non-identical ligand.

Deuteration shifts of the order of 40–100 cm^{-1} can be quantified from room temperature absorption spectra. Fig. 17 shows the absorption spectrum and the shift between the $x=0$ and $x=3$ materials. The ^{1}MLCT band shows a blue shift of about 40 cm^{-1}. This is the same value as seen for the ^{3}MLCT origins but does not imply that the ^{1}MLCT excitations are localised. Put simply, a delocalised excitation will have an identical average shift of corresponding localised (protonated and deuterated) excitations and broadband spectroscopy is unable to discriminate. The higher energy π–π^* excitations show a shift more than twice that of the MLCT excitations. Features marked π_1 and π_2 (Fig. 17) can be identified as ligand centred rather than MLCT in nature simply from their deuteration shift.

5.5. Ligand substitution and three-level patterns

Neither the excited state lifetimes nor the characteristic I–II and I–III spacings of ruthenium complexes vary greatly with the specific environment of the chromophore (Table 1). Energy level spacings are similar in heteroleptic complexes where one,

two or three ligands are directly involved in the MLCT luminescence. In the $[Ru(bpy)_{3-x}(phen)_x]^{2+}$ ($x=0$ to 3) series [83] it was possible to very clearly identify energy spacings associated with both Ru–bpy and Ru–phen subunits which again varied little in the series.

The situation in the intense ^{1}MLCT region is different. Splittings of 100–1000 cm^{-1} occur and spectra can vary markedly from environment to environment. For example, the absorption spectrum in the ClO_4 lattice is markedly different to that obtained in solution or more symmetric environments [16]. The lack of sensitivity of the ^{3}MLCT sublevels to spatial symmetries is consistent with a spin-only, ^{3}A characteristic of the lowest ^{3}MLCT emitting levels and not a ^{3}E orbital parentage which will naturally split in the presence of a low-symmetry field. The anisotropy of the Zeeman rotation patterns can be quantitatively analysed within a localised model.

A comparison of the radiative lifetimes of I, II and III in $[Ru(bpy)_3]^{2+}$ with oscillator strengths calculated from integrated molar extinction values in the broadband triplet region indicates [16] that much of the absorption intensity in the region is due to these three transitions, but is dominated by level III, the most intense. By far the greatest part of the intensity is associated with broadband structures and very little (<1%) with the electronic origins I, II and III.

The intensity of the origins increases greatly in the ClO_4 crystals without significant changes in the overall broadband structures that carry the bulk of the intensity or luminescence lifetimes. This confirms that the broadband structure is vibronically induced in nature with the intensity in the origin regions originating from a different (static) mechanism. MCPL studies helped establish that broadband luminescence in $[Ru(bpy)_3]^{2+}$ from the characteristically non-degenerate states I, II and III is vibronically induced in nature [81]. The vibronic bandshape is markedly different for the three states.

The situation in third-row (Os, Ir, Re) MLCT emitting complexes is different. Temperature-dependent lifetime studies on a series of osmium and rhenium compounds in Table 1 indicate a far greater spread of effective energy gaps. The iridium systems discussed in Section 5.1 also show variable I–II gaps, indicative of more orbital contribution to these levels. Spin–orbit coupling for Os(II) is of the order of 3000 cm^{-1} and becomes a dominant influence. The distinction between nominally ^{3}MLCT and ^{1}MLCT regions is marginal in third-row metal complexes. There is also considerably more absorption intensity polarised out of the metal–ligand plane which is not expected for MLCT excitations and different theoretical approaches may be called for.

5.6. *Vibrational sideline patterns*

Electronic excitations of a complex, whether metal-centred, ligand-centred or charge transfer, involve some charge redistribution. Vibrational modes of the complex are coupled to electronic excitations and will appear as sidelines in the luminescence or excitation spectra. Laser selective spectroscopy can greatly enhance the ability to observe and identify sidelines. This occurs because vibrational frequencies

Table 1
Compendium of energy spacings (cm^{-1}) of ^{3}MLCT luminescent states

Chromophore	Δ_{I-II}	Δ_{I-III}	Host	Method	References
$[Ru(bpy)_3]^{2+}$	8.6	62.1	$[Zn(bpy)_3](ClO_4)_2$	Direct	[59], [60][a]
$[Ru(bpy)_3]^{2+}$	8.7	55	$[Zn(bpy)_3](ClO_4)_2$	Lifetime fit	[61]
$[Ru(bpy)_3]^{2+}$	6.9	61	$[Ru(bpy)_3](PF_6)_2$	Direct	[16], [57]
$[Ru(bpy)_3]^{2+}$	8.8	67	Poly(vinyl alcohol)	Lifetime fit	[81]
$[Ru(bpy)_3]^{2+}$	8.1	68	$[Zn(bpy)_3](PF_6)_2$	Lifetime fit	[82]
$[Ru(bpy)_2(4,4'\text{-}(CO_2C_2H_5)_2\text{-}bpy)]^{2+}$	9.8	70.8	4:1 Ethanol/methanol	Lifetime fit	[81]
$[Ru(phen)_3]^{2+}$	6	34	$[Zn(bpy)_3](ClO_4)_2$	Direct	[83]
$[Ru(bpy)_2(phen)]^{2+}$	8.5	61	$[Zn(bpy)_3](ClO_4)_2$	Ru-bpy, direct	[83][b]
$[Ru(bpy)_2(phen)]^{2+}$	5.7	32.7	$[Zn(bpy)_3](ClO_4)_2$	Ru-phen, direct	[83][b]
$[Ru(bpy)(phen)_2]^{2+}$	6.0	33.5	$[Zn(bpy)_3](ClO_4)_2$	Ru-phen, direct	[83]
$[Ru(phen)_3]^{2+}$	6.7	54	4:1 Ethanol/methanol	Lifetime fit	[84]
$[Ru(bpy)_2phen]^{2+}$	7.6	59	4:1 Ethanol/methanol	Lifetime fit	[84][c]
$[Ru(bpy)(phen)_2]^{2+}$	6.7	53	4:1 Ethanol/methanol	Lifetime fit	[84][c]
$[Ru(bpy)_2(bpz)]^{2+}$	18	98	$[Zn(bpy)_3](ClO_4)_2$	Direct	[71]
$[Ru(bpy)_2(bprid)]^{2+}$	15.5/8.4	96/89	$[Zn(bpy)_3](ClO_4)_2$	Direct equiv/dist	[70][d]
$[Ru(bpy)(bprid)_2]^{2+}$	13.2	75	$[Zn(bpy)_3](ClO_4)_2$	Direct	[70]
$[Ru(bprid)_3]^{2+}$	7.5	60	$[Zn(bpy)_3](ClO_4)_2$	Direct	[70]
$[Ir(bpy)_2(acac)]^{2+}$	9/15	200?	4:1 Ethanol/methanol	Lifetime/narrow	[61][e]
$[Ir(bpy)_2(MeOH)_2]^{3+}$	5/8	200?	4:1 Ethanol/methanol	Lifetime/narrow	[61][e]
$Re(bpy)(CO)_3Cl$	6.3	90.4	EPA glass	Lifetime fit	[85]
$Re(4,4'\text{-}Me_2bpy)(CO)_3Cl$	4.5	75.7	EPA glass	Lifetime fit	[85]
$Re(phen)(CO)_3Cl$	14.0	42.1	EPA glass	Lifetime fit	[85]
$Re(2,9\text{-}Me_2phen)(CO)_3Cl$	4.5	75.7	EPA glass	Lifetime fit	[85]
$[Os(bpy)_3]^{2+}$	≈60	?	$[Ru(bpy)_3](PF_6)_2$	Direct/average	[86][f]
$[Os(bpy)_3]^{2+}$	≈105	?	$[Zn(bpy)_3](ClO_4)_2$	Direct/average	[68], [87][f]
$[Os(bpy)_3]^{2+}$	16	52	Poly(methyl methacrylate)	Lifetime fit	[88]
$[Os(4,4'\text{-}Me_2bpy)_3]^{2+}$	42	119	4:1 Ethanol/methanol	Lifetime fit	[88]
$[Os(phen)_3]^{2+}$	23	63	Poly(methyl methacrylate)	Lifetime fit	[88]
$[Os(5,6\text{-}Me_2phen)_3]^{2+}$	42	119	Poly(methyl methacrylate)	Lifetime fit	[88]
$[Os(4,7\text{-}Me_2phen)_3]^{2+}$	34	173	Poly(methyl methacrylate)	Lifetime fit	[88]
$[Os(bpy)_2(bprid)]^{2+}$	53,43	?	$[Zn(bpy)_3](ClO_4)_2$	Direct equiv/dist	[89][g]

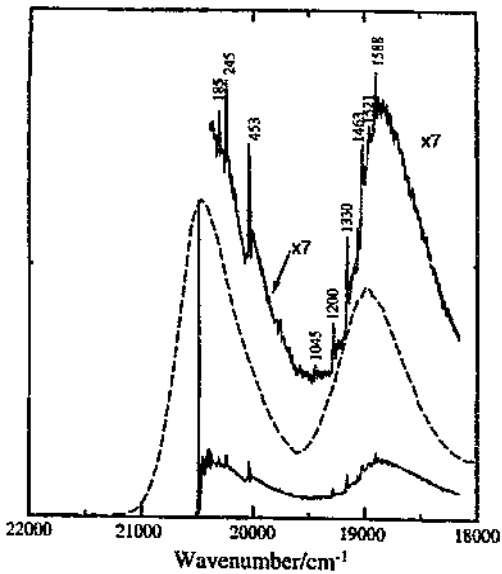

Fig. 18. Non-resonantly excited (at 457.9 nm) and FLN spectra (excited at 488.0 nm) of $[Ir(5,6\text{-}Me_2phen)_2Cl_2]^+$ in glycerol at 1.5 K. Adapted from [25].

are, in general, well correlated and narrowing of an electronic origin feature also leads to sharpening of sideline features. Fig. 18 shows the vibrational sideline features that can be seen after narrowing into a featureless luminescence spectrum of $[IrCl_2(5,6\ Me_2phen)_2]^+$ in frozen solution.

The degree to which any particular mode is coupled reflects the nuclear displacement between the ground and a particular excited electronic state along the normal coordinate of that specific mode. Such coupling information can, at least in principle, provide information regarding excitation localisation in an excited state. A π–π^* excitation in a complex couples strongly to the modes of the ligand undergoing the

---

[a]Previous measurements [59] obtained a larger Δ_{I-II}. At low temperatures, nanoheterogeneity and excitation transfer lead to an apparent shift of level I to lower energies. This is also evident in the shift [56] of origin II between absorption and luminescence measurements in $[Ru(bpy)_3](PF_6)_2$.

[b]Energy spacings for both Ru–bpy and Ru–phen subunits can be measured for heteroleptic materials.

[c]Values obtained are somewhat intermediate to values for $[Ru(phen)_3]^{2+}$ and $[Ru(bpy)_3]^{2+}$ systems. Nanoheterogeneity will ensure that these systems have will have a range of Ru–bpy and Ru–phen luminescent ^{3}MLCT subunits.

[d]Spacings corresponding to luminescence of the Ru–bprid subunit for the ligand in either the equivalent or distinct ligand position could be identified.

[e]Different values of the average energy gap are obtained by either a lifetime analysis or direct narrowing as the I–II gap in this system is not well correlated.

[f]The I and II levels are split by exciton coupling. The values given are those extrapolated to no exciton coupling.

excitation, but may couple less strongly to metal–ligand and modes of other (spectator) ligands. Metal-centred excitations couple to metal–ligand modes and, to a lesser extent, ligand modes.

The MLCT process is characterised as a two-centre excitation and we may expect that both metal–ligand and ligand modes be significantly coupled. When a ^{3}MLCT excitation is localised on a single metal–ligand subunit, as happens in ruthenium complexes, it is important to recognise that the spectator ligands see the metal core being reduced in the emission process, i.e. changing from Ru(III) to Ru(II). Sidelines associated with the spectator modes will reflect this change in the interaction of the central metal with the ligand. Back bonding of bpy with Ru(II) is strong, but weak with Ru(III). Thus there will be a distinct change of metal–π^* interaction between ground and excited states. The mere appearance of vibrational sidelines associated with spectator ligands in a luminescence spectrum does not imply delocalisation of ^{3}MLCT states.

This is demonstrated [70] in the luminescence spectrum of $[Ru(bpy)_2(bprid)]^{2+}$ in $[Zn(bpy)_3](ClO_4)_2$. The ^{3}MLCT state is localised on the bprid ligand, yet vibrational sidelines associated with the bpy ligands are coupled. Indeed, the most intense sideline in the low frequency range is the 477 cm^{-1} bpy mode.

Sidelines in the luminescence spectra of the $[Ru(bpy)_{3-x}(bpy\text{-}d_8)_x]^{2+}$ in $[Zn(bpy)_3](ClO_4)_2$ series reveal a similar pattern [70]. Both deuterated and protonated modes are observed in the $x=1$ system although the lowest excited state is localised on an Ru–bpy subunit. Similarly, both deuterated and protonated modes appear in the $x=2$ system. However, emission from an Ru–bpy-d_8 subunit shows substantially stronger coupling to deuterated modes than emission which arises from an Ru–bpy subunit.

A further complication is the different intensities of sideline patterns for the same chromophore in different lattices studied [71]. This sensitivity obfuscates a simple interpretation of sideband structures. There is also a sensitivity to the central metal. Fig. 19 compares the sidelines of $[Ru(bpy)_2(bpz)]^{2+}$ with those of $[Ru(bpy)_3]^{2+}$ and $[Os(bpy)_3]^{2+}$ in $[Zn(bpy)_3](ClO_4)_2$. The 1443 cm^{-1} bpy mode is intense in the $[Os(bpy)_3]^{2+}$ spectrum and practically absent in the $[Ru(bpy)_3]^{2+}$ spectrum. Deuteration studies establish that the 1123, 1244, 1443 and 1569 cm^{-1} modes in $[Ru(bpy)_2(bpz)]^{2+}$ are due to the spectator bpy ligands.

The 1495 cm^{-1} bpy mode is missing in the spectrum of $[Ru(bpy)_2(bpz)]^{2+}$. The intensity of this mode is remarkably variable. It is also absent in the emission of $[Os(bpy)_3]^{2+}$ in the $[Ru(bpy)_3](PF_6)_2$ host, whereas it corresponds to the most prominent mode in the emission of the same complex in $[Zn(bpy)_3](ClO_4)_2$. It is absent in the emission of the $[Os(bpy)(bpy\text{-}d_8)_2]^{2+}$ chromophore in the $[Zn(bpy)_3](ClO_4)_2$ host when the complex enters the lattice with both bpy-d_8 ligands in the crystallographically equivalent ligand positions. It is also missing in the luminescence from the Ru–bpy-d_8 subunits in $[Ru(bpy)(bpy\text{-}d_8)_2]^{2+}$ in $[Zn(bpy)_3](ClO_4)_2$. The 1495 cm^{-1} mode appears to fingerprint when the bpy ligand is not a spectator and is directly involved in the ^{3}MLCT emission.

Careful (solution-based) ground and excited state resonance Raman work has been performed [90] on $[Ru(bpy)_2(bpz)]^{2+}$ and other systems [91]. In the excited

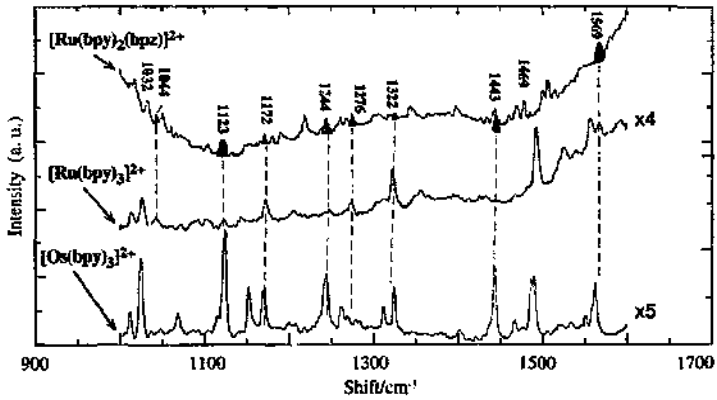

Fig. 19. Vibrational sidelines patterns in the high-frequency region for the chromophores indicated, obtained by displacing the lowest origin feature of their luminescence spectra doped in $[Zn(bpy)_3(ClO_4)_2]$ to zero. Origin features have normalised intensity. Adapted from [71].

state, modes associated with the bpz anion and spectator "neutral" bpy modes were identified, supporting the original Raman assignments.

5.7. *Intramolecular excitation transfer*

Luminescence of $[Ru(bpy)_3]^{2+}$ in $[Zn(bpy)_3](ClO_4)_2$ involves two independent but crystallographically equivalent metal–ligand subunits $Ru–L_b$ and $Ru–L_{b'}$ (see Fig. 11). The inhomogeneous broadening of the origins varies from sample to sample, but is approximately 3–10 cm^{-1}. As outlined in previous sections, the I–II and I–III spacings are well correlated within a subunit but excitations on the different subunits correlate poorly.

When narrow band excitation is used to excite the system on the higher energy side of the inhomogeneously broadened profile of an origin, a sharp feature is seen along with the broader feature at low energy. With excitation on the lower energy side, no broad feature is seen in luminescence. Thus, intramolecular excitation transfer occurs between the two metal–ligand subunits. When the temperature is low compared to the energy spread in the inhomogeneous broadening of the MLCT excitation, the excitation transfer process will be predominantly to metal–ligand subunits at lower energy.

At 2 K, the relaxation from level III is fast ($\tau \approx 10$ ps) as determined by its homogeneous linewidth (1.1 cm^{-1}) in narrowing experiments. The relaxation rate from II to I is far slower ($\tau = 210$ ns). An experiment to directly measure [92] the intramolecular excitation transfer rate is initiated by short pulse (10 ns) narrow bandwidth (0.05 nm) laser excitation into the high-energy side of origin III at 1.8 K. This initial excitation is followed by a rapid radiationless conversion to level II, which is metastable. As levels III and II are well correlated, a narrowed emission is observed at λ_1 (the high-energy side of origin II) even at the shortest observation

times after excitation. At later times, luminescence on the low-energy side of the inhomogeneously broadened origin II (i.e. around λ_2 in Fig. 20) builds up, when excitation transfer processes to the Ru–L_b, subunit have become important. The time-resolved spectra and intensity transients at specific detected wavelengths show that excitation transfer occurs on the 10–20 ns timescale. Similar results are obtained for excitation transfer between the two Ru-bpy-d_8 subunits in $[Ru(bpy)(bpy\text{-}d_8)_2]^{2+}$.

The excitation energy transfer from Ru–bpy-d_8 to Ru–bpy subunits where the energy gap is about 40 cm^{-1} is much faster. This is a consequence of the far higher density of phonon states of the lattice for this energy difference. Excitation transfer must be accompanied by phonon emission to ensure energy conservation. The very small mismatch of 1–5 cm^{-1} arising from inhomogeneity for homologous subunits is at least partially responsible for the relatively slow (10–20 ns) intramolecular excitation transfer process observed.

Kelley and co-workers have observed [93,94] intramolecular transfer kinetics for both $[Ru(bpy)_3]^{2+}$ and $[Os(bpy)_3]^{2+}$ in solution via transient absorption spectroscopy. The results are influenced by solvent properties in a rather complex fashion and average transfer times are in the range of 30–200 ps. As experiments were performed at room temperature, the rates will be dominated by those in levels II and III.

5.8. *Intramolecular exciton behaviour in Os(II) systems*

As mentioned in Section 5.2, $[Os(bpy)_3]^{2+}$ doped in $[Ru(bpy)_3](PF_6)_2$ luminesces from the three $C3$ sites of the host. The excitation exchange coupling between the three equivalent Os–bpy subunits, quantified by the parameter β, is small but measurable from splittings in spectral features as -2.3 cm^{-1}. The coupling is

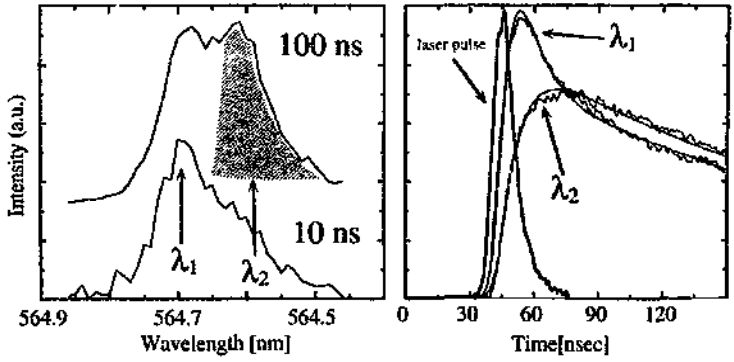

Fig. 20. Some results obtained from the excitation transfer experiment in the lowest energy excitations in $[Zn(bpy)_3(ClO_4)_2]$:Ru outlined in Fig. 15. Left-hand panel shows the time-dependent narrowing evident with a rise in intensity occurring near λ_2 after 10 ns. The corresponding kinetics detected at λ_1 and λ_2 are shown in the right-hand panel. The solid lines are fits to the kinetics (see [92]).

substantially less than the deuteration shift (32 cm^{-1}) and a very nice pattern develops in the spectroscopy [87] of the lowest-excited states in the series $[Os(bpy)_{3-x}(bpy\text{-}d_8)_x]^{2+}$ doped in this lattice. The threefold mini-exciton is broken by deuteration into a twofold unit and a remaining fully localised excitation.

The $x=0$ and $x=3$ systems show a 7 cm^{-1} (3β) splitting of the lowest origin I. Coupling of three Os–bpy subunits gives rise to an E level and a dipole-forbidden A level. As the lower component is very weak, A is lower than E, which determines the sign of β. In the $x=1$ system the lowest energy feature is an excitonic structure split by 2β and corresponds to two coupled Os–bpy subunits. In the $x=2$ system, localisation on the lone Os–bpy subunit occurs in the lowest state. Fig. 21 shows excitation and luminescence spectra for the series for the lowest excitations of the lowest energy site.

Nanoheterogeneity in this lattice is comparable to β. An important consequence of this is that spectral features associated with two or three coupled ligands cannot be substantially narrowed. This can be used as a fingerprint for weakly coupled excitons where the excitation exchange interaction is of the same order of magnitude as the nanoheterogeneity. We have performed a range of Stark experiments on these systems. An applied electric field of about 10^5 V cm^{-1} can effectively localise the mini-exciton.

Fig. 22 shows the absorption and luminescence spectra of the same series doped in the $[Zn(bpy)_3](ClO_4)_2$ lattice in the region of the electronic origins. Whereas the $x=0$ and $x=3$ systems have a single origin in luminescence, the $x=1$ and $x=2$ systems show two [88,89]. Origins can be systematically assigned to the complexes

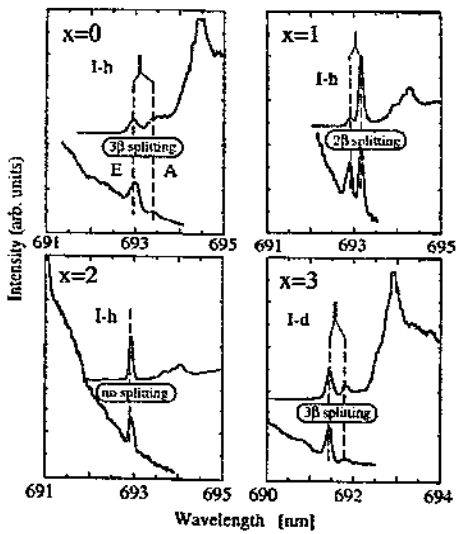

Fig. 21. Resonantly narrowed luminescence and excitation spectra of the series $[Os(bpy)_{3-x}(bpy\text{-}d_8)_x]^{2+}$ in $[Ru(bpy)_3(PF_6)_2]$ at 4.2 K. Adapted from [86].

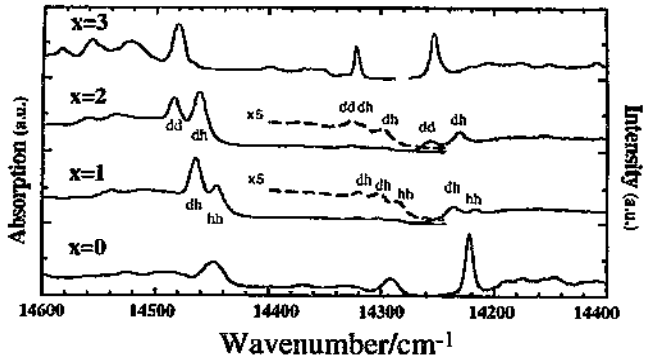

Fig. 22. Luminescence and absorption spectra of the series $[Os(bpy)_{3-x}(bpy\text{-}d_8)_x]^{2+}$ in $[Zn(bpy)_3(ClO_4)_2]$. Adapted from [87].

which enter the lattice by substituting the crystallographically equivalent ligands with two bpys, or one bpy-d_8 and one bpy or two bpy-d_8s. These species are abbreviated as h-h, d-h and d-d, respectively. Corresponding assignments can be made in absorption spectra.

In contrast to the same chromophore in the PF_6 lattice, the excitation exchange parameter β must be (at least) of the same order of magnitude as the deuteration shift. This follows from the origins of the d-h species being about halfway between the position for the $x=0$ and $x=3$ systems. Four origins can be identified for each species. Polarised absorption spectra (Fig. 23) help demonstrate that O2 and O4 are Davidov components arising from the exciton coupling of two equivalent metal–ligand units in level II and have the expected intensity ratio of 1:3. The spectroscopy of the entire series can be very well accounted for in terms of a simple exciton formalism with an excitation exchange interaction of $\beta \approx 79$ cm^{-1} in level II and 37.5 cm^{-1} in level I.

In the $[Ru(bpy)_3](PF_6)_2$ lattice levels I and II of $[Os(bpy)_3]^{2+}$ are separated by 60 cm^{-1} Both levels are split by a small exciton splitting of $3|\beta| = 7$ cm^{-1}. In the $[Zn(bpy)_3](ClO_4)_2$ lattice, excitation exchange splittings are 40–80 cm^{-1} and comparable to the deuteration shift. In the former system deuteration leads to localisation, but does not occur in the latter.

6. Conclusions

Laser selective spectroscopy, especially those experiments performed on high-symmetry crystal lattices, have been invaluable in advancing our understanding and quantifying a number of important concepts. For MLCT systems, the $C2/c$ perchlorates are a particularly invaluable environment. The influence of the anion environment on the charge transfer excitations, rather than changes in the chromophore geometry itself, is a dominant factor creating an internal Stark effect that breaks

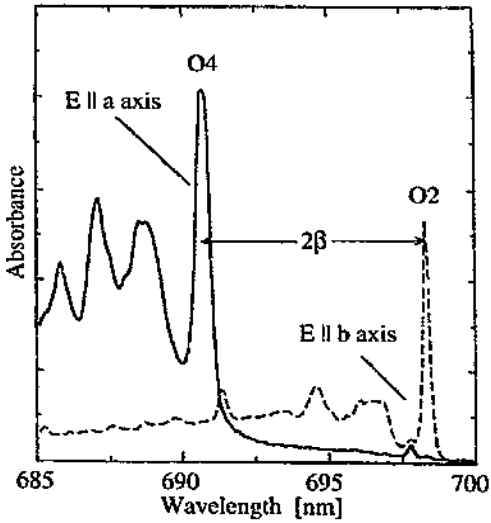

Fig. 23. Polarised absorption spectrum (in the metal–ligand plane) of the lowest energy features of $[Os(bpy\text{-}d_8)_3]^{2+}$ doped in $[Zn(bpy)_3(ClO_4)_2]$. Adapted from [68].

the trigonal symmetry of the chromophore in a well-defined way. Their low inhomogeneous linewidths, along with the ability to measure polarised spectra, provide us with a level of detail that forms a basis of a new spectroscopic analysis of the MLCT systems.

From the experimental evidence, the mere presence or absence of specific vibrational modes cannot be indiscriminately used to determine whether a ^{3}MLCT state is delocalised or localised.

Theoretical estimates of excitation coupling of both metal–ligand and ligand-centred excitations in trigonal chromophores have been consistently too large, by orders of magnitude or more. Excitation transfer between crystallographically equivalent metal–ligand units in $[Ru(bpy)_3]^{2+}$ can be as slow as about 10 ns. This corresponds to a excitation exchange value β of about 10^{-3} cm^{-1} using ν=4 J h^{-1}. Excitation coupling of the lowest electronic states of $[Os(bpy)_3]^{2+}$ is of the order of 2–30 cm^{-1} but is seen to be markedly sensitive to the environment. The variability of apparent energy gaps, as measured from temperature dependent lifetime data in frozen solutions for third-row metal ^{3}MLCT emitters, can be understood on this basis.

Nanoheterogeneity leads to both ligand-centred and metal–ligand exciton basis states (Fig. 5) losing resonance. Termed diagonal disorder, the independent inhomogeneous spread is about 1–20 cm^{-1} in crystalline lattices but is 1–2 orders of magnitude greater in amorphous environments such as frozen solutions. ^{3}MLCT luminescent levels of osmium(II) complexes in amorphous environments remain most likely to be localised on a single metal–ligand subunit as the excitation exchange interaction cannot overcome the influence of nanoheterogeneity.

A bright future remains for laser selective spectroscopy. Our application of FLN and hole-burning methods reported present only a fraction of the armoury of techniques of laser spectroscopy and we look forward to the application of some of these to a range of systems of chemical interest.

Acknowledgements

We would like to thank Dr Lynne Wallace for her contributions in many of these studies and Professor D.P. Craig for his interest in this work.

References

[1] D.A. Bardwell, F. Barigelletti, R.L. Cleary, L. Flamigni, M. Guardili, J.C. Jeffery and M.D. Ward, Inorg. Chem., 34 (1995) 2438.
[2] H. Riesen and E. Krausz, Comments Inorg. Chem., 14 (1993) 283.
[3] H. Riesen and E. Krausz, Comments Inorg. Chem., 18 (1995) 395.
[4] J. Ferguson, F. Herren, E. Krausz, M. Maeder and J. Vrbancich, Coord. Chem. Rev., 64 (1985) 21.
[5] T.J. Meyer, Pure Appl. Chem., 58 (1986) 1193.
[6] R.A. Krause, Struct. Bonding (Berlin), 67 (1987) 2.
[7] E. Krausz, Comments Inorg. Chem., 7 (1988) 139.
[8] A. Juris, F. Barigelletti, S. Campagna, V. Balzani, P. Belser and A. von Zelewsky, Coord. Chem. Rev., 84 (1988) 85.
[9] E. Krausz and J. Ferguson, Prog. Inorg. Chem., 37 (1989) 293.
[10] H. Yersin and D. Braun, Coord. Chem. Rev., 11 (1991) 39.
[11] C. Daul, E.J. Baerends and P.Vernooijs, Inorg. Chem., 33 (1994) 3538.
[12] B. Bosnich, Inorg. Chem., 7 (1968) 178.
[13] S.F. Mason and B.J. Norman, Chem. Phys. Lett., 2 (1968) 22.
[14] R.G. Bray, J. Ferguson and C.J. Hawkins, Aust. J. Chem., 22 (1968) 2091.
[15] J. Ferguson, E. Krausz and J. Vrbancich, Chem. Phys. Lett., 131 (1986) 463.
[16] E. Krausz, H. Riesen and A.D. Rae, Aust. J. Chem., 48 (1995) 929.
[17] J. Ferguson and F. Herren, Chem. Phys., 76 (1983) 45.
[18] H. Riesen, E. Krausz and M. Puza, Chem. Phys. Lett., 151 (1988) 65.
[19] D.H. Oh and S. Boxer, J. Am. Chem. Soc., 111 (1989) 1130.
[20] I.B. Talanina, M.A. Collins, L. Dubicki and E. Krausz, Chem. Phys. Lett., 200 (1992) 318.
[21] H. Riesen and E. Krausz, J. Lumin., 53 (1992) 263.
[22] H. Riesen and E. Krausz, Chem. Phys. Lett., 172 (1990) 5.
[23] H. Riesen and E. Krausz, Chem. Phys. Lett., 182 (1991) 266.
[24] H. Riesen, E. Krausz, A. Zilian and H.-U. Güdel, Chem. Phys. Lett., 182 (1991) 271.
[25] H. Riesen, E. Krausz and L. Wallace, J. Phys. Chem., 96 (1992) 3621.
[26] J. Westra and M. Glasbeek, J. Lumin., 53 (1992) 92.
[27] H. Riesen and E. Krausz, Optical Society of America Technical Digest, 16 (1991) 82.
[28] M.K. DeArmond and C.M. Carlin, Coord. Chem Rev., 36 (1981) 325.
[29] R.J. Watts and G.A. Crosby, J. Am. Chem. Soc., 93 (1971) 3184.
[30] R.J. Watts, G.A. Crosby and J.L. Sansregret, Inorg. Chem., 11 (1972) 1474.
[31] R.J. Watts, T.P. White and B.G. Griffith, J. Am. Chem. Soc., 97 (1975) 6914.
[32] R. Ballardini, G. Varani, L. Moggi, V. Balzani, K.R. Olson, F. Scandola and M.Z. Hoffman, J. Am. Chem. Soc., 97 (1975) 728.
[33] R.J. Watts, B.G. Griffith and J.S. Harrington, J. Am. Chem. Soc., 98 (1976) 674.
[34] R. Ballardini, G. Varani, L. Moggi and V. Balzani, J. Am. Chem. Soc., 99 (1977) 6881.

[35] R.J. Watts and D. Missimer, J. Am. Chem. Soc., 100 (1978) 5350.
[36] R.J. Watts, S. Efrima and H. Metiu, J. Am. Chem. Soc., 101 (1979) 2742.
[37] Y. Ohashi and T. Kobayashi, Bull. Chem. Soc. Jpn., 52 (1979) 2214.
[38] B. Divisia, P.C. Ford and R.J. Watts, J. Am. Chem. Soc., 102 (1980) 7264.
[39] R.J. Watts, Inorg. Chem., 20 (1980) 2302.
[40] J. DiBenedetto, R.J. Watts and P.C. Ford, Inorg. Chem., 23 (1984) 3039.
[41] G.A. Crosby and W.H. Elfring, Jr., J. Phys. Chem., 80 (1976) 2206.
[42] (a) P.J. Giordano, S.M. Fredericks, M.S. Wrighton and D.L. Morse, J. Am. Chem. Soc., 100 (1978) 2257. (b) S.M. Fredericks, J.C. Luong and M.S. Wrighton, J. Am. Chem. Soc., 101 (1979) 7415.
[43] A. Juris, S. Campagna, I. Bidd, J.-M. Lehn and R. Ziessel, Inorg. Chem., 27 (1988) 4007.
[44] J.R. Shaw and R.H. Schmehl, J. Am. Chem. Soc., 113 (1991) 389.
[45] R.M. Leasure, L. Sacksteder, D. Nesselrodt, G.A. Reitz, J.N. Demas and B.A. DeGraff, Inorg. Chem., 30 (1991) 3722.
[46] L. Sacksteder, M. Lee, J.N. Demas and B.A. DeGraff, J. Am. Chem. Soc., 115 (1993) 8230.
[47] L. Wallace and D.P. Rillema, Inorg. Chem., 32 (1993) 3836.
[48] L. Wallace, C. Woods and D.P. Rillema, Inorg. Chem., 34 (1995) 2875.
[49] G. Ferraudi, M. Feliz, E. Wolcan, I. Hsu, S.A. Moya and J.J. Guerrero, J. Phys. Chem., 99 (1995) 4929.
[50] E. Krausz, J. Higgins and R. Riesen, Inorg. Chem., 32 4053 (1993).
[51] H. Riesen and E. Krausz, J. Chem. Phys., 97 (1992) 7902.
[52] L. Wallace, G.A. Heath, E. Krausz and G. Moran, Inorg. Chem., 30 (1992) 347.
[53] E. Gallhuber, G. Hensler and H. Yersin, Chem. Phys. Lett., 120 (1985) 445.
[54] G. Hensler, E. Gallhuber and H. Yersin, Inorg. Chim. Acta, 113 (1986) 91.
[55] H. Yersin, E. Gallhuber and G. Hensler, Chem. Phys. Lett., 134 (1987) 497.
[56] E. Krausz, Chem. Phys. Lett., 135 (1987) 249.
[57] H. Riesen and E. Krausz, Chem. Phys. Lett., 151 (1988) 71.
[58] Y. Komada, S. Yamauchi and N. Hirota, J. Phys. Chem., 92 (1988) 6511.
[59] M. Kato, S. Yamauchi and N. Hirota, Chem. Phys. Lett., 140 (1989) 543.
[60] H. Riesen and E. Krausz, Chem. Phys. Lett., 212 (1993) 347.
[61] H. Riesen and E. Krausz, J. Lumin., 62 (1994) 253.
[62] D.P. Rillema, D.S. Jones and H.A. Levy, J. Chem. Soc., Chem. Commun., (1979) 849.
[63] M. Biner, H.B. Bürgi, A. Ludi and C. Röhr, J. Am. Chem. Soc., 114 (1992) 5197.
[64] D. Braun, E. Gallhuber, G. Hensler and H. Yersin, Mol. Phys., 67 (1989) 417.
[65] H. Riesen, A.D. Rae and E. Krausz, J. Lumin., 62 (1994) 123.
[66] J.M. Harrowfield and A.N. Sobolev, Aust. J. Chem., 47 (1994) 763.
[67] U. Klement, D. Trümbach and H. Yersin, Z. Krist., 210 (1995) 228.
[68] H. Riesen, L. Wallace and E. Krausz, Mol. Phys., 87 (1996) 1299.
[69] H. Riesen, L. Wallace and E. Krausz, Proc. 1st Australian Conf. on Vibrational Spectroscopy, 1995, p. 167.
[70] H. Riesen, L. Wallace and E. Krausz, Chem. Phys., 198 (1995) 269.
[71] H. Riesen, L. Wallace and E. Krausz, J. Phys. Chem., 100 (1996) 4390.
[72] H. Riesen and E. Krausz, J. Lumin., 58 (1994) 176.
[73] H. Riesen and E. Krausz, Chem. Phys. Lett., 217 (1994) 613.
[74] S. Yamauchi, Y. Komada and N. Hirota, Chem. Phys. Lett., 129 (1986) 197.
[75] H. Yersin, D. Braun, G. Hensler and E. Gallhuber, NATO ASI Ser., Ser. C, 288 (1989) 95.
[76] H. Yersin, E. Gallhuber, G. Hensler and D. Schweitzer, Chem. Phys. Lett., 161 (1989) 315.
[77] D. Braun, D. Schweitzer and H. Yersin, J. Phys. Chem., 93 (1989) 7555.
[78] H. Riesen and E. Krausz, J. Chem. Phys., 99 (1993) 7614.
[79] H. Riesen and E. Krausz, J. Lumin., 66–67 (1996) 496.
[80] H. Riesen, L. Wallace and E. Krausz, J. Phys. Chem., 99 (1995) 16807.
[81] E. Krausz and G. Moran, J. Chem. Phys., 90 (1989) 39.
[82] E. Krausz and G. Moran, J. Lumin., 42 (1988) 21.
[83] H. Riesen, L. Wallace and E. Krausz, Chem. Phys Lett., 228 (1994) 605.
[84] W.H. Elfring, Jr., and G.A. Crosby, J. Am. Chem. Soc., 103 (1981) 2687.

[85] D.R. Stripling and G.A. Crosby, Chem. Phys. Lett., 221 (1994) 426.
[86] H. Riesen, L. Wallace and E. Krausz, J. Chem. Phys., 102 (1995) 4823.
[87] H. Riesen and E. Krausz, in Jai Singh (Ed.), Excitonic Processes in Condensed Matter, Proc. SPIE 2362, Bellingham, WA, 1995, p. 408.
[88] D.E. Lacky, B.J. Pankuch and G.A. Crosby, J. Phys. Chem., 84 (1980) 2068.
[89] L. Wallace, H. Riesen and E. Krausz, unpublished results.
[90] G.D. Danzer and J.R. Kincaid, J. Phys. Chem., 94 (1990) 3976.
[91] G.D. Danzer, J.A. Golus and J.R. Kincaid, J. Am. Chem. Soc., 115 (1993) 8643.
[92] H. Riesen, Y. Gao and E. Krausz, Chem. Phys. Lett., 228 (1994) 610.
[93] R.A. Malone and D.F. Kelley, J. Phys. Chem., 95 (1991) 8970.
[94] J.L. Pogge and D.F. Kelley, Chem. Phys. Lett., 238 (1995) 16.